Turbulent Combustion of Carbon-free Fuels I- Mini Review of Spherically Expanding Premixed Turbulent Ammonia Flames

Seif Zitouni, Pierre Brequigny, Christine Mounaïm-Rousselle

■SERIAL LECTURE■

- English Title (not required) -

Mini Review of Spherically Expanding Premixed Turbulent Ammonia Flames

ZITOUNI, **Seif**, **BREQUIGNY**, **Pierre**, **and MOUNAIM-ROUSSELLE, Christine**[1]

Université Orléans, INSA-CVL, EA 4229 – PRISME, Orléans F-45072, France

1 Institut Universitaire de France, IUF, Paris, France

Abstract: Ammonia is recognized as a potential hydrogen carrier but increasingly as a carbon free fuel for all energy applications. However, significant challenges exist in ammonia combustion due to its low flammability, low burning intensity and the potential for high detrimental emissions. This mini review article focuses on the state of the art in understanding the specifics of turbulence-flame interaction of partially cracked and uncracked ammonia in the expanding spherical flame configuration. The paper highlights the need for experimental data coupled with DNS to develop useful modeling tools that accurately predict the specific response of the ammonia flame to the turbulence front.

Key words : Ammonia, Premixed combustion, Spherically expanding flames, Turbulence-flame interaction

1. Introduction

Ammonia is increasingly been recognized not just as a hydrogen carrier but as a carbon-free fuel in its own right [1]. Despite notable progress in the power sector, especially with Gas Turbines (GT) [2] Internal Combustion Engines (ICE) [3], and more recently, industrial burners [4], the use of ammonia in combustion systems continues to pose challenges. These difficulties are mainly due to the intrinsic combustion characteristics and the potential emissions it may produce. Issues such as ammonia's slow burning velocity, narrow flammability range, and high ignition energy often result in reduced burning efficiency, flame instability, and difficulties with flame extinction in practical systems [5–7]. Most review papers concluded that to address some of these challenges, one promising strategy is the 'on board' production of hydrogen to enhance ammonia combustion. This is obtained by a cracking system (thermal, electric or plasma) to partially crack ammonia. The addition of hydrogen in all combustion technologies enhances flame properties like ignition and the flame development process.

The use of ammonia, either alone or blended with hydrogen, in combustion technologies requires significant advancements in the combustion process. In fact, even for hydrocarbon fuels, combustion remains one of the least understood physical processes. This is because combustion occurs at the interface between turbulence - a complex, nonlinear phenomenon in fluid mechanics - and chemistry, which, despite ongoing research, is still not fully understood and involves high activation energy chemistry. For the past fifty years, a major effort of combustion research has focused on turbulence-flame interaction studies, by identifying key governing parameters, to accelerate science-based predictive capabilities, to guide design, operation, and fuel formulation for practical combustion devices.

Although significant progress has been made with traditional fuels such as hydrocarbons, the validation and/or the improvement of these models must now be expanded to new zero-carbon fuels, e.g., ammonia (NH_3), hydrogen (H_2), or various synthetic fuels that may exhibit very different flame characteristics and thermo-diffusive properties compared to conventional carbon-based fuels, especially as the shift to a zero-carbon future accelerates.

The fundamental concepts of turbulence-flame interaction, based on the pioneering works such as those of Lewis and von Elbe [8], Borghi [9], Peters [10] and Williams [11], have been refined through advances in theoretical understanding, more sophisticated optical diagnostics and direct numerical simulations, increasingly valuable due to the exponential increase in computing power. However, when focusing specifically on ammonia, the current state of knowledge on complex interaction between fluid dynamics, molecular transport and combustion chemistry in flames is still in its early stages.

The turbulent flame speed is crucial for the operation of both ICE and GT. In ICE, it controls the burning rate, while in GT, it influences the flame angle relative to the flow, thereby affecting the flame location. Over the past few decades, turbulent flame speed measurements have been performed using different experimental set-ups and fuels. The configuration of the expanding turbulent flames (Fig. 1) is of significant interest, as the flame surface and the enhancement of flame speed are influenced solely by turbulent vortices, rather than by a mean flow and there is no local impact on the stabilization process as in turbulent jet.

Under turbulent conditions, symmetrically distributed fans (as indicated in orange in Fig. 1) create a central zone where

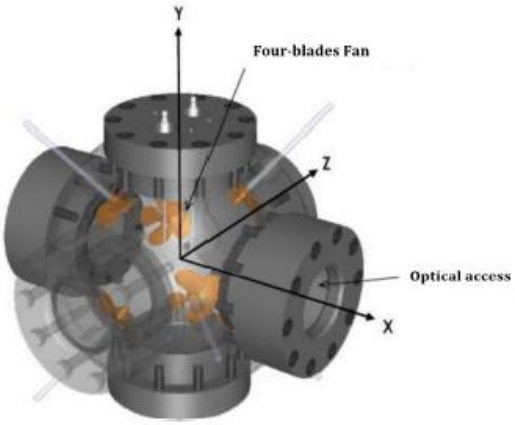

Fig.1 Schematic of a spherical combustion chamber.

the turbulence is considered homogeneous and isotropic. For spherically expanding flames, Bradley et al. [12], introduced the notion that the unburnt gas volume inside a sphere is equal to the burnt volume outside it. This reference is used to estimate the turbulent burning velocity, approximating the turbulent flame propagation as if it is a planar flame front. In this approach, both the mass and entrainment turbulent burning velocities are considered equal. Therefore, the instantaneous turbulent flame propagation is defined as the instantaneous turbulent burning velocity multiplied by the expansion ratio, estimated as $S_T = \sigma dR_f/dt$, with R_f, the flame radius extracted from the flame images assuming spherical shapes and σ the expansion ratio.

Turbulence is characterized in such flow fields by the turbulence intensity, u' and the integral length scale, L_T. The turbulent intensity is proportional to the fan speed, whilst L_T is dependent upon the vessel size [13] and the blade pitch angle of the fans [14]. However, while there is a clear relation between the propagation speed of a laminar flame front and its stretch rate, the acceleration mechanism of turbulent expanding flames is more complex. As discussed extensively in the literature [15,16], there is no universally agreed-upon definition for characterizing the propagation of turbulent flame, with uncertainty arising from experimental and measurement techniques as well as varying flow conditions. Several scaling laws for turbulent flame speeds, normalized by the laminar burning unstretched velocity, S_L^0, have been suggested as summarized in [17] to provide a universal formula to predict the dependence of turbulent flame speed on basic turbulence and mixture characteristics.

Due to the different but complementary fundamental characteristics of ammonia and hydrogen, partially cracked ammonia (NH_3/H_2 or $NH_3/H_2/N_2$ mixture) can provide different hydrogen concentrations to enhance the burning velocity in comparison with 100% NH_3 and to control it in comparison with 100% H_2. Only a few studies exist on the use of $NH_3/(H_2+N_2)$ blends when operating under turbulent conditions of interest and at temperature and pressure more representative of realistic systems, as can be seen in Table 1.

This paper therefore reviews recent insights into the turbulent flame behavior of ammonia-based fuels from experimental and numerical results obtained by Direct Numerical Simulations (DNS) in the context of freely expanding flames. The review is structured as follows: first, it covers the characteristics of turbulence-flame interactions, turbulent flame speed correlations and finally it discusses local flame structures.

Table 1 – Summary of literature review – All references below employ the spherically expanding flame configuration (Ω, O_2 content in O_2+N_2, n = fan)

Authors (Year) [Ref]	Mixture Composition	Equivalence Ratio (Φ)	Pressure Unburnt (P_u)	Temperature Unburnt (T_u)	u' (m/s)	L_T (mm)
Xia et al. (2020) [18]	NH_3/air (Ω = 0.4)	0.6 – 1.6	1 bar	298 K	0 – 1.29	20.9
Hashimoto et al. (2021) [19]	NH_3-CH_4 (0 – 100%)	0.4 – 1.7	1 bar	298 K	0 – 5.80	20.9
Wang et al. (2021) [20]	NH_3/air (Ω = 0.25 – 0.4)	1.0	0.1 – 0.3 MPa	298 K	0.78 – 2.34	~ 23
Lhuillier et al. (2021) [21]	NH_3, NH_3/H_2, NH_3/CH_4 (up to 15% H_2 or CH_4)	0.9	0.54 MPa	445 K	1.04 – 1.73	3.4
Dai et al. (2022) [22]	NH_3/CH_4 (20,40,60% NH_3)	1.0	1 – 3 bars	298 K	0.91 – 2.72	$16.44(1\text{-}0.99^n)$
Dai et al. (2023) [23]	NH_3/H_2 (50,80% NH_3)	0.8, 1.0, 1.3	1 – 5 atm	298 K	0.91 – 2.72	$16.44(1\text{-}0.99^n)$
Wang et al. (2023) [24]	NH_3/H_2 (40,50,60% NH_3)	0.6, 0.9	1 – 5 bars	373 K	0.78 – 2.34	~ 23
Zitouni et al. (2023) [25]	NH_3, NH_3/H_2, NH_3/CH_4 (up to 60% H_2 or CH_4)	1.0	1 bar	298 K 423 K (NH_3)	0 – 0.82	2.6
Zitouni et al. (2024) [26]	NH_3/H_2, (5 – 50% H_2) $NH_3/H_2/N_2$ (5 – 40% PCA)	0.8,1.0,1.2	1 bar	298 K	0 – 1.13	2.6
Cao et al. (2024) [27]	NH_3/H_2 (60,40,20% NH_3)	1.0	0.1 – 0.3 MPa	298 K	0.85 – 2.53	9.2 – 16.9

2. Turbulent Flame Speed of NH_3

2.1 Turbulent Combustion Regime

The fundamental characteristics of laminar ammonia combustion, such as the unstretched laminar flame speed (S_L^0) and laminar flame thickness (δ_L), are key parameters that play an important role on the turbulent combustion processes. In the case of ammonia flames, S_L^0 peaks at $\Phi \sim 1.05–1.1$, with a value around 7 cm/s [28–30]. Under oxygen enhanced combustion, 40% O_2 (Ω = 0.40, Ω= O_2 content in O_2+N_2) results in a five-fold increase in NH_3 S_L^0, with laminar burning velocities comparable to those of CH_4 [31]. Furthermore, it is interesting to notice that NH_3 exhibits closer pressure exponents to zero than CH_4, whilst displaying higher temperature exponents than those of CH_4 [29,32]. As such, it seems higher temperatures and pressures would be considered desirable for practical combustion systems.

When H_2 is blended with ammonia or simulated through partially 'cracked' ammonia (PCA) mixtures (NH_3/H_2/N_2), S_L^0 increases exponentially as the H_2 content rises, with $S_{L\,max}^0$ shifting towards richer fuel conditions. A 40% H_2 addition (or 30% of PCA) results in S_L^0 values similar to CH_4 [26,33]. Ammonia exhibits a significantly thicker laminar flame, with the preheat zone being 3 to 4 times thicker and the reaction zone 5 to 6 times thicker compared to that of CH_4 or H_2. However, a small addition of H_2 (20%) results in decreasing the flame thickness by half.

Due to the very distinctive characteristics of NH_3 flames, including low S_L^0 and large flame thickness, significant differences in timescales relative to hydrocarbon flames lead to different flame responses to the turbulence as highlighted in Fig.2. Zitouni et al. [26] and Wang et al. [24] observed that after the dissipation of initial ignition energy, NH_3 flames lose their spherical shape and develop elongated “tube” or “strip” shapes, as shown in Fig. 2 (a - c). They attributed this to the slow laminar burning velocity of NH_3, noting that increasing the NH_3 content slows down the flame speed. As the time to reach the same flame radius increases the impact of gravity becomes more significant, leading to thicker flames and greater instability. Yang et al. [34] noted ‘smoother flame structures’ were observed under rich conditions compared to lean conditions, a finding also supported by DNS work from Mukundakumar et al [35], shown in Fig 2 (d). Under turbulent conditions, intrinsic laminar flame instabilities (hydrodynamic and/or preferential-diffusional) interact with

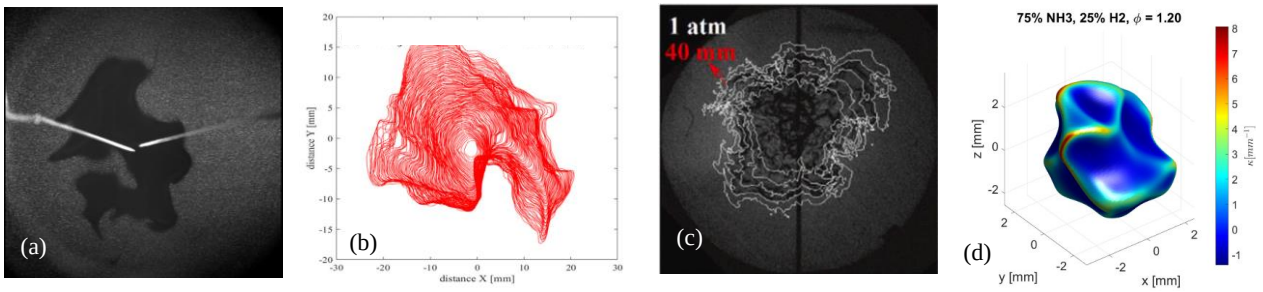

Fig.2 (a) NH_3/air flame (u’=0.82, Φ = 1) [25], (b) flame contour of NH_3/air (u’=0.82, Φ = 1) [25], (c) flame contour of NH_3/air (u’=0.78, Φ = 1, Ω = 0.25) [20], (d) 2D DNS profile of 75% NH_3 – 25% H_2 flame (Φ = 1.20) [35]

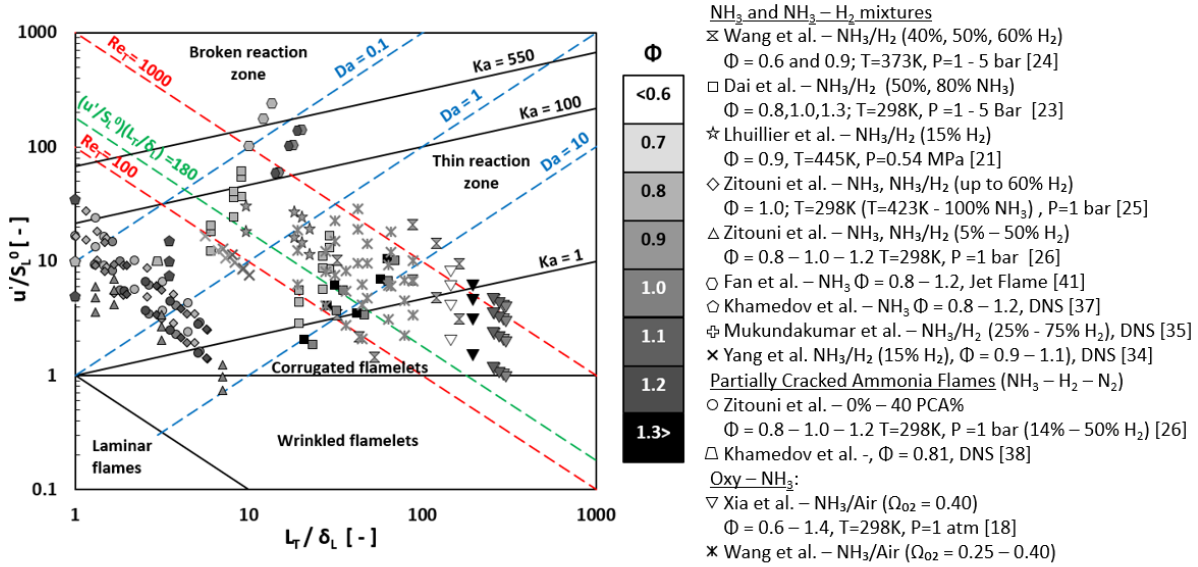

Fig. 3 Literature NH_3-based fuels and DNS on the Peter-Borghi diagram.

the disturbance effects of multi-scale turbulent eddies, modifying and increasing small-scale flame stretching and wrinkling, which accelerates the flame. Ichimura et al. [36] investigated the extinction characteristics of pure NH_3/air flames and found that although the maximum $S_L°$ for NH_3 is at $\Phi \approx 1.05$, leaner mixtures, particularly at $\Phi = 0.9$, provide better resistance to turbulence-induced extinction compared to richer mixtures. The authors highlighted the potential thermo-diffusive accelerating effects of lean NH_3/mixtures, which exhibited Le slightly below 1.

The structures of turbulent premixed flames are commonly classified into different regimes of combustion, with the boundaries of these regimes classically delimitated by parameters such as Damköhler (Da), Karlovitz (Ka), and turbulent Reynolds Number (Re_T), with Da referring to the ratio of the rate of chemical reaction to mass transport, expressed as $Da = (S_L^0/u').(L_T/\delta_L)$ and Ka, the ratio of chemical to turbulent time scale, $Ka = (\delta_L/S_L^0)/(L_T/u')$. Fig. 3 illustrates the positioning of the various NH_3-based literature experimental data and those from selected DNS [34,35,37,38] studies on the Peters- Borghi diagram [39]. Most of these published datasets fall within the thin reaction ($1 < Ka < 100$) or the corrugated (wrinkled) flamelet regime zone. In these regimes, while the flame surface is significantly deformed, it still maintains flamelet behavior for large eddies. Small-scale eddies can penetrate the preheat zone, enhancing mass and heat transfer rates, which broaden or 'thicken' the turbulent flame brush. However, the reaction zone remains thin and unaffected by the eddy motion, preserving a laminar structure [39]. Skiba et al. [40] proposed that flame thickening occurs when the turbulent diffusivity (u'/S_L^0) exceeds the molecular diffusivity (L_T/δ_L) by a factor of 180 within the preheat layer. Their experimental results conducted at high turbulence (Ka = 550) showed no broken or distributed reaction layers. Both these boundaries are depicted in Fig. 3. The only NH_3 study to fall within this high turbulence zone is that of Fan et al. [41]. Their results indicate that even at Ka = 1000, the thin NH reaction layer (considered to represent the fuel consumption zone) is not broadened by small-scale eddies. This suggests that the thin reaction zone theory may still be applicable to ammonia/air flames at high Ka (Ka >> 100). Other studies [42] suggest that flame thickening could affect both the preheat and reaction sheets beyond this boundary. However, it remains uncertain whether the flame broadening phenomenon occurs in spherical expanding flames. This has an expected consequence on turbulent flame speed enhancement by H_2 or O_2, as will be discussed later.

2.2 Turbulent Propagation Speed

The initial flame front is can only be wrinkled by the smallest sized eddies, smaller than the flame size, continually growing until the flame kernel incorporates the entire turbulence spectrum [43]. As such, the flame propagation speed is expected to reach a plateau at some point. It is of interest to note that even for large combustion vessels, in most of the studies no clear distinct plateau experimental data [21,26,43–46] is reached, as can be seen in Fig. 3(a). Therefore, the experimental determination of S_T needs to consider other definitions. The value of S_T is considered as the average of the quasi-linear increase of dR_f/dt, by taking the slope of best-linear fit [44], directly by taking into account the time differentiation [45], or as the last possible measurable value (at the maximum of radius [21,43]), while Wu et al. [46] introduced a volume-averaged S_T expression (S_{Tmean}), also used by Wang et al. [24]. Last, in the case of freely-expanding flames, Lipatnikov and Chomiak [47] argued that the extrapolating S_T values as a function of global stretch rate ($K_{global} = 0$) might provide a more universal estimate of S_T.

Xia et al. [18] studied turbulent O_2-enriched NH_3 combustion, as displayed in Fig. 3(b) illustrating the results of S_T and $S_L°$ from lean to rich conditions at various u' (0. 32 –

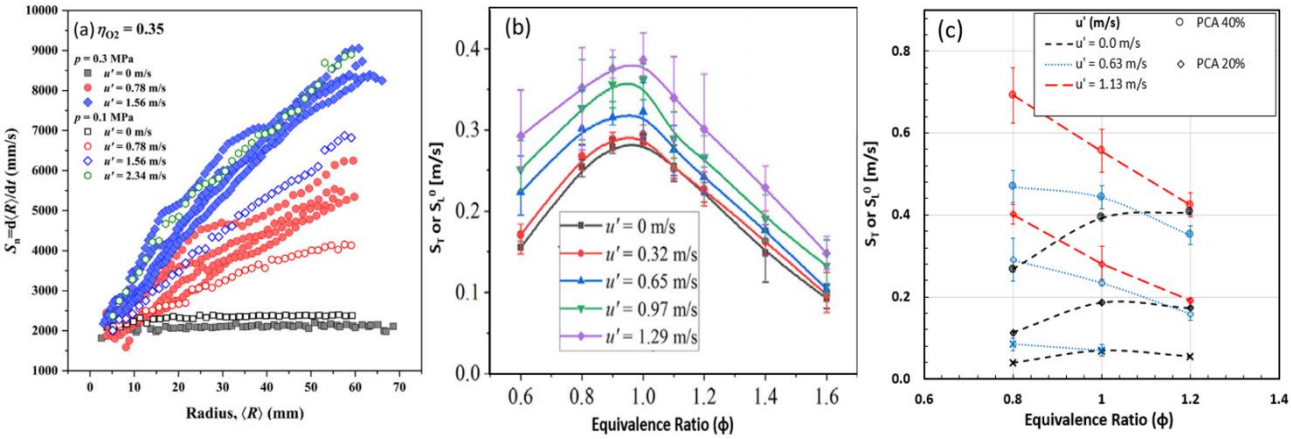

Fig.4 (a) Turbulent flame speed as a function of mean flame radius with increasing u' and P at 298 for O_2 = 0.35 [20] Turbulent of laminar flame speed as a function of equivalence ratio for (b) NH3/air (O_2 = 0.40) [18] and (c) Partially Cracked Ammonia ($NH_3/H_2/N_2$), at 298 K and 1 bar [26]

1.29 m/s). Increasing u' yields enhanced flame speed, attributed to an increase in the flame surface area. The typical bell-curve shape of S_L^0 as function of Φ is maintained. The authors noted that the ratio of turbulent to laminar flame speed (S_T/S_L^0) increases more significantly under lean conditions than under rich conditions, at a given u'. This was attributed to preferential diffusion, as lean O_2-NH_3 mixtures have lower Le values than rich mixtures: for Ω = 0.40, Le = 0.94 at Φ = 0.6 and 1.08 at Φ = 1.6). Wang et al. [48] also studied oxygen enriched NH_3 flames under elevated pressures (0.1-0.3MPa) and varying u' (0.78 – 2.34 m/s). They concluded that the S_T/S_L^0 ratio decreased with increasing O_2 content, primarily due to an increase in S_L^0 rather than S_T.

Regarding H_2 enrichment to NH_3 flames, Fig 3 (c) illustrates the S_T and S_L^0 trends in the case of PCA flames. As expected, even if the content of N_2 in the PCA acts as a small addition of diluent, similar trends are observed for binary NH_3/H_2 flames [26]. Lean mixtures exhibit highest S_T, which decreases as Φ increases for a fixed turbulent intensity, consistent with other studies [23,24]. This behavior contrasts trends observed in the case of oxy-enriched NH_3 combustion at it can be seen in Fig.3(b) [31]. Indeed, at rich conditions, S_T values are closer to the corresponding S_L^0 values, with some cases showing slower flame speeds, without the much-expected increase in flame speed due to the turbulence, at least under weak u' < 0.65 m/s (Fig 3c). A similar behavior is observed for a $50NH_3/50H_2$, mixture at Φ = 1.3 and u' = 0.91 m/s as reported in [23].

Lhuillier et al.[21] first observed that up to 10-15% H_2 enrichment in NH_3, the normalized turbulent flame speed increases due to the enhancement of molecular diffusivity provided by H_2. However, further enrichment leads to a "bending" response, where the normalized S_T decreases with increasing H_2 content. This decrease in S_T/S_L^0 with increasing H_2 content was also observed in other studies [23,24,26].Yang et al. [34], performing DNS with detailed chemistry, investigated turbulent, spherically expanding NH_3/H_2 flames under similar unburnt conditions and turbulence intensities as in [21]. They also observed the bending effect for S_T/S_L^0 at approximately 10% H_2, not only in lean but also in stoichiometric and rich conditions. Various explanations were proposed, notably regarding the position of such flames on the Peters-Borghi diagram. Zitouni et al. [26] suggested that this "bending" occurs for ammonia flames near the Ka = 100 limit, marking the transition from the thin reaction to the broken reaction regime. In this latter regime, the smallest Kolmogorov eddies can both thicken the flame and penetrate the reaction zone structure. At this limit, it has been theorized that reaction layers may become broken or distributed, however this seems unlikely considering the results of [41].

The measured trends in turbulent flame speed are typically explained through a combination of preferential-diffusion (Le) or stretch-related behavior represented by L_b, the burning Markstein length, which accounts for the enhanced (or reduced) burning rate under lean (or rich) conditions [23,26,31,47,48]. For spherically expanding flames, the outward propagation leads most flamelet to exhibit positive curvature, resulting in positive stretch rate. Thus, when $L_b<0$ (as Le<1), which is the case for lean NH_3 (Φ≤0.8), NH_3-H_2 blends (Φ≤0.8) and O_2-enriched NH_3 flames (Φ≤0.7), the turbulent flamelet experiences accelerated flame propagation, a process that is further enhanced with increasing turbulence. This is somewhat supported by the work of Khamedov et al. [37] who used DNS to investigate the propagation behaviour of turbulent, premixed NH_3 and blends with H_2 and N_2 flames (Φ = 0.81 and 1.2). For rich NH_3-based flames, the peaks of the probability density function (PDF) for local flame speed displacement and curvature are smaller than the corresponding laminar values, resulting in reduced turbulent flame propagation. In contrast, for lean flames, the peaks match the laminar values, indicating an increased turbulent flame speed. These findings are consistent with experimental trends observed in [23,26,31,36,48]. Finally, regarding the influence of pressure, increasing the initial pressure reduces the viscosity, which in turn increases the Reynolds number, leading to an enhancement in turbulent flame speed. This effect has been observed in both oxy-NH_3 combustion [48] and NH_3-H_2 blends [23].

2.3 Scaling lows for Turbulent Propagation Speed

Recent studies [21,23,24,26,31,48] have strived to find a scaling law for S_T of NH_3-based fuels. This type of universal correlation remains useful for 0-1D engineering modelling tools. Several expressions of of S_T/S_L^0have been evaluated with different parameters such as u', S_L^0, δ_L, L_T, Le or Ma, where Ma is the Markstein number, i.e. the ratio of L_b to δ_L or also characteristic combustion properties, Ka and Da.

For O_2 – enriched NH_3 flames, Xia et al. [31] proposed a linear relationship between Ka and S_T/S_L^0. However, despite the significant uncertainty, the authors noted that the results for the leanest (Φ = 0.6) and richest (Φ = 1.6) mixtures deviate from this relationship due to a combination of preferential diffusional effects (Φ = 0.6) and lower flame temperatures (Φ = 0.8). Dai et al. [23], building on the work of Kiagawa et al. [49], who showed that $S_T/S_L^0 \sim (Re \cdot Le^{-2})^a$ for lean H_2 flames, proposed a modified version of the Bradley et al. correlation [50]. The new formulation $S_T/S_L^0 = a(Re_{T,flame} \cdot Le^{-2})^b$, replaces the Reynolds number (Re) with the turbulent flame Reynolds number (Re_{Tflame}, evaluated with respect to the radius), which

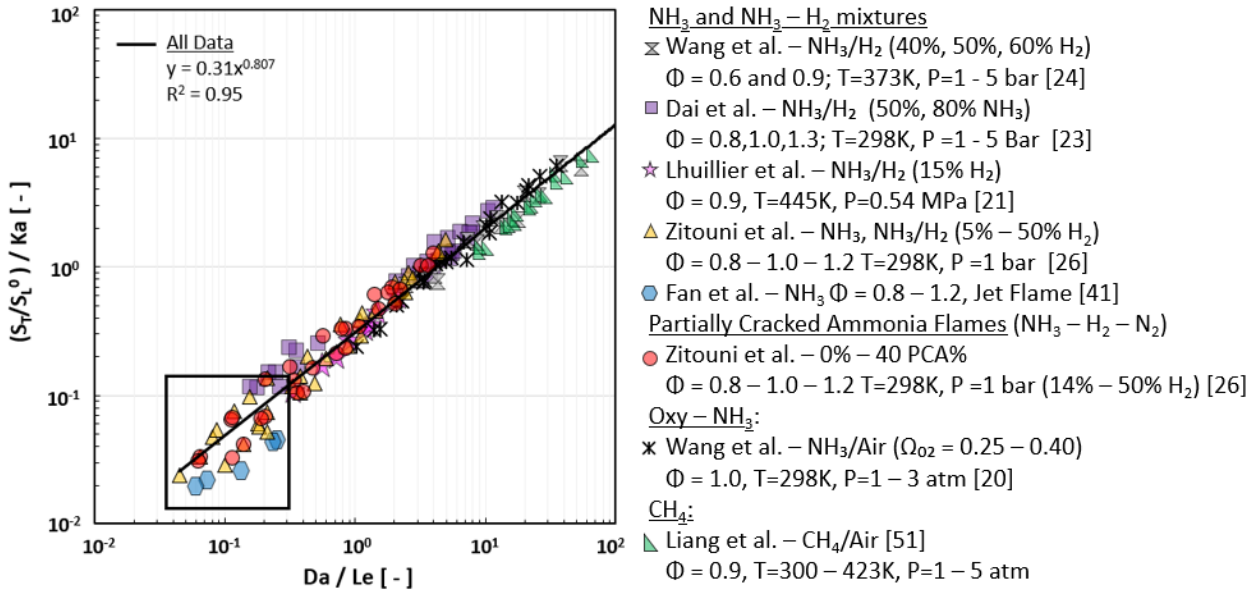

Fig.5 Correlation of S_T in the form of S_T/S_L^0 /Ka = $A(Da/Le)^B$.

better accounts for the self-similar characteristics of spherical expanding flames. These modified correlations showed good agreement between NH_3/H_2 and syngas/air flames. Lhuillier et al. [21] introduced a correlation based upon Da corrected S_T/S_L^0 against Ka, while Wang et al. [24] revised this by incorporating the influence of Le, resulting in the expression S_T/S_L^0/Ka = $A(Da/Le)^B$, where A and B are equal to 0.37 and 0.81, respectively. Fig. 5 demonstrates this correlation against NH_3-based literature data, all employing spherically expanding flames (except [41]), across a range of temperatures and pressure (as indicated in the legend) and of L_T (~2.64–45 mm). The datasets also include the CH_4 data from Jiang et al. [51] as a baseline for comparison, along with experimental NH_3/air jet-flame data from Fan et al. [41] at high Ka (Ka > 100). As can be seen from Fig.5, a very good correlation is observed, collapsing well into the empirical formulation, with the pre-factor and constant values matching those reported in [24,26].

For cases where Ka >> 1 and Da << 1 (e.g. H_2 < 15%; Φ = 0.8 -1.0 [26], and Jet NH_3/air flames[41]), indicated by the black square in Fig. 5, significant deviations are observed. DNS data from [52] suggest that the classical power exponents of scaling laws in the form of $S_T/S_L^0 = (u'/S_L)^a(L_T/\delta_L)^b$ are mainly controlled by the transition from different combustion regimes (Da <<1 to Da >> 1). The lower the Da the more pronounced dependence of S_T/S_L^0 on L_T/δ_L, transitioning from $S_T/u' \sim Da^{0.5}$ to $S_T \sim u'$, for Da <<1 to Da >>1, respectively; this effect potentially contributing to the differences observed for Da<<1, in Fig. 5. Moreover, the different mixtures exhibit very different turbulent and chemical times scales, leading to distinct global and local flame structures which will be further discussed in the following section.

3. Global and local Flame structure of NH_3

Any change in initial conditions, such as turbulence, initial conditions, mixture, ultimately affects the flame characteristics. At the local level, these changes are particularly evident on the flame surface, influencing phenomena such as flame stretching, wrinkling, and curvature distribution. Ichimura et al. [36] and Hashimoto et al. [19] investigated turbulent flame propagation limits of NH_3 and the relationship with Ka. Both studies conclude that at Φ = 0.9, NH_3/air (as well as O_2-enriched NH_3 and NH_3/CH_4) flames exhibited best resistance to induced turbulent extinction and could withstand highest Ka, at room temperature and pressure. They attributed this behavior to the changes in stretch (Ma or L_b) and preferential diffusion (Le). However, it remains important to note that even for low addition of H_2, Le remains around 1, and that the measured L_b trend keeps on decreasing after Φ = 0.9, which should theoretically enhance resistance to stretch-induced extinction. There is, however, a trade-off between S_L^0 and Ma. While several experiments [19,28,30] observed a decrease in L_b with decreasing Φ, recent DNS work [53] and theoretical analysis [30] suggest a non-linear L_b-relationship with Φ with a minimum point at Φ=0.9, which aligns with the experimental findings of Ichimura et al. and Hashimoto et al. [19,36]. Recent zero-gravity tests [54], which eliminate buoyancy, also reveal stretch-dependency patterns similar to those predicted by theory [30] and DNS studies [53].

In [25], where the average wrinkling flame ratio of NH_3 and NH3-H_2 blends was examined, it was observed that at the

lowest turbulence intensity, all flames exhibited similar wrinkling ratios, suggesting similar flame structures. However, at higher u', flames with higher NH_3 content exhibited a sharper increase in the wrinkling ratio, as illustrated in Fig. 6(a). Wang et al. [24] and Xia et al. [18] also confirmed that for constant equivalence ratio, pressure, and hydrogen (or oxygen) content, increasing u' intensifies the wrinkling due to stronger turbulence, which reduces the Taylor and Kolmogorov scales. Yang et al. [34] observed fewer wrinkles under rich conditions compared to lean conditions, a finding that was confirmed by DNS studies conducted by Mukundakumar et al [35]. Overall, factors such as NH_3 content, O_2 content, turbulence intensity, equivalence ratio, and pressure influence the surface flame wrinkling.

Zitouni et al. [25] used Mie-scattering tomography to investigate the mean flame curvature by averaging local curvature values along the flame front. They observed that the mean flame curvature decreases from positive to an asymptotic value near zero over time. As the flame expands, the ratio of convex (positive curvature) to concave (negative curvature) fronts balances. They noted that all investigated blends exhibit similar levels of dispersion in terms of average curvature and standard deviation, regardless of the turbulence intensity (u'), suggesting similar wrinkling instabilities. On a local level, Zitouni et al. [55] analyzed changes in the probability density function (PDF) of local curvature distribution for NH_3 and its blends with H_2 or CH_4, as presented in Fig. 6(b). They showed that trends in wrinkling agree well with local curvature PDF, with an increase in u' resulting in a decrease in the peak and a widening of the PDF, with average curvature slightly > 0. It is also noticed that a non-monotonous trend in PDF peak as a function of H_2 addition, as illustrated in Fig. 6b.

Based on DNS, Mukundakumar et al. [35] and Yang et al. [34] also analyzed changes in the PDF of local curvature distribution for NH_3 and NH_3/H_2, as illustrated in Fig. 6c. They found the greatest spread in the PDF for flames with the highest NH_3 content, indicating that although the flame surface is wrinkled, the curvature radius is large, meaning the curvature values are small. For a constant amount of H_2, as the equivalence ratio increases, the spread of curvature increases as well, suggesting that small wrinkles with low curvature are smoothed out, leading to strongly curved, highly strained flame fronts. These observations can be explained by the preferential diffusion effects of H_2. As the H_2 content increases, the preferential diffusion effects enhance, distorting the flame surface more. Increasing the global equivalence ratio (especially in stoichiometric and rich cases) forces the local equivalence ratio to reach richer levels, reducing the

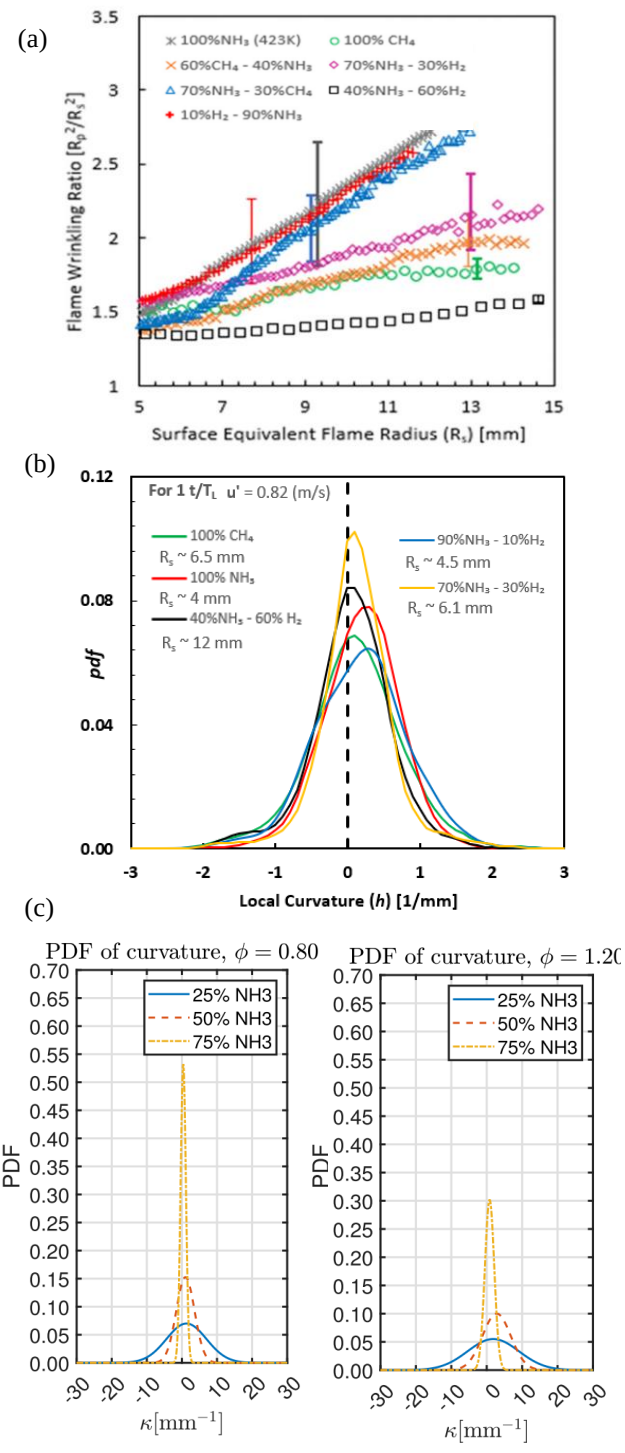

Fig. 6 (a) Flame wrinkling ratio as a function of flame radius, u' = 0.82 [25], (b) Probability density functions of curvature at 1 eddy turn over time for various NH3-based mixtures, u' = 0.82 [55], (c) Probability density functions of curvature for Φ = 0.8 and (h) Φ = 1.2 of NH_3-H_2 blends [35]

flame speed at points on the surface, smoothing out small-scale wrinkles. It must be pointed out that for these last results the amount of H_2 is very high from 25% to 75% on vol, enhancing the influence of specific H_2 behaviour. Despite these findings, local flame analysis of NH_3-based flames remains limited, with significant research gaps regarding the

interaction between the flame front and turbulence, flame morphology, and local turbulent flame structure.

3. Conclusions

This mini-review paper offers an overview of the current state of turbulent combustion research concerning ammonia-based fuels, using the spherical expanding flame configuration. While significant advancements have been made in understanding NH_3 combustion, several challenges persist. To further enhance our comprehension of ammonia combustion, there is a need for more high-fidelity simulations that can better clarify the interactions between the flame front and turbulence. Additionally, further experimental investigations under high-pressure conditions are required, essential for developing more accurate combustion models at practical application relevant conditions. Lastly, the development of advanced combustion concepts that more effectively capture the distinct characteristics of ammonia combustion remains a critical area for future research.

Acknowledgments

Some of the results presented in this paper were derived from work funded by European Union's Horizon 2020 research and innovation programme agreement No. 884157, by the French Government ANR-11- LABX-0006–01 and ANR-22-CE50-0022.

References

[1] David W. I. F., *et al., JPhys Energy* 6 (2024).

[2] Pashchenko, D., *Energy* 290: 130275 (2024).

[3] Qi, Y., Liu, W., Liu, S., Wang, W., Peng, Y., and Wang, Z., *eTransportation* 18: 100288 (2023).

[4] Valera-Medina, A., *et al., Int. J. Hydrogen Energy* 49: 597–1618 (2024).

[5] Elbaz, A. M., Wang, S., Guiberti, T. F., and Roberts, W. L., *Fuel Commun.* 10: 100053 (2022).

[6] Kobayashi, H., Hayakawa, A., Somarathne, K. D. K. A., and Okafor, E. C., *Proc. Combust. Inst.* 37: 109–133 (2019).

[7] Herbinet, O., Bartocci, P., and Grinberg Dana, A., *Fuel Commun.*11: 100064 (2022).

[8] Lewis, B. and Von Elbe, G., *Combustion, flames and Explosions of gases*. New York: Academic Press, (1961).

[9] Borghi, R., *Recent Advances in the Aerospace Sciences: In Honor of Luigi Crocco on His Seventy-fifth Birthday*, 117–138 (1985).

[10] Peters, N., *Meas. Sci. Technol.*12: 2022 (2001).

[11] Williams, F. A., *Combust. Flame* 26: 269–270 (1976).

[12] D. Bradley *et al., Combust. Flame* 133: 415–430 (2003).

[13] Leisenheimer, B., and Leuckel, W., *Combust. Sci. Technol.*: 118, 147–164 (1996).

[14] Ravi, S., Peltier, S. J., and Petersen, E. L., *Exp. Fluids* 54:(2013).

[15] Lipatnikov, A. N., and Chomiak, J., *Prog. Energy Combust. Sci.* 28: 1–74 (2002).

[16] Driscoll, J. F., *Prog. Energy Combust. Sci.*, 34: 91–134 (2008).

[17] Burke, E. M., Güthe, F., and Monaghan, R. F. D., *Proceedings of the ASME Turbo Expo.*, 4B: (2016).

[18] Xia, Y., *et al., Fuel* 268: 117383 (2020).

[19] Hashimoto, G., *et al., Proc. Combust. Inst.* 38: 5181–5190 (2021).

[20] Wang, S., Elbaz, A. M., Wang, Z., and Roberts, W. L., *Combust. Flame* 232: 111521 (2021).

[21] Lhuillier, C., Brequigny, P., Contino, F., and Mounaïm-Rousselle, C., *Proc. Combust. Inst.* 38: 6671–6678 (2021).

[22] Dai, H., Wang, J., Cai, X., Su, S., Zhao, H., and Huang, Z., *Combust. Flame* 242: 112183 (2022).

[23] Dai, H., Wang, J., Cai, X., Su, S., Zhao, H. and Huang, Z., *Proc. Combust. Inst.* 39: 1689–1697, (2023).

[24] Wang, S., Elbaz, A. M., Arab, O. Z., and Roberts, W. L., *Fuel* 332: 126152 (2023).

[25] Zitouni, S., Brequigny,P., and Mounaïm-Rousselle, C., *Proc. Combust. Inst.* 39: 2269–2278, (2023).

[26] Zitouni, S., Bréquigny, P., and Mounaïm-Rousselle, C., *Fuel Commun.* 20: 100126 (2024).

[27] Bin Cao, J., Ma, J.Q., Li, G.X., Li, H. M., and Jiang, R.P., *Energy and Fuels* 38: 17965-17977 (2024).

[28] Hayakawa, A., Goto, T., Mimoto, R., Arakawa, Y., Kudo, T., and Kobayashi, H., *Fuel* 159 98–106 (2015).

[29] Kanoshima, R., *et al., Fuel* 310 122149 (2022).

[30] Zitouni,S., Brequigny, P., and Mounaïm-Rousselle, C., *Combust. Flame* 253: 112786 (2023).

[31] Xia Y., *et al., Fuel* 268: 117383 (2020).

[32] Hayakawa, A., Nagaoka, T., Kosada, H., Takeishi, H., Kudo, T., and Nakamura, H., *Proc. Combust. Inst.* 40: 105778 (2024).

[33] Mei, B., Zhang, J., Shi, X., Xi, Z., and Li, Y., *Combust. Flame* 231: 111472 (2021).

[34] Yang, W., Ranga Dinesh, K. K. J., Luo, K. H., and Thevenin, D., *Int. J. Hydrogen Energy* 47:11083–11100 (2022).

[35] Mukundakumar, N. and Bastiaans, R., *Energies* 15:134749 (2022).

[36] Ichimura, R., Hadi, K., Hashimoto, N., Hayakawa, A., Kobayashi, H., and Fujita, O., *Fuel* 246: 178–186 (2019).

[37] Khamedov, R., Song, W., Hernández-Pérez, F. E., and Im, H. G., *Flow, Turbul. Combust.* (2023).

[38] Khamedov, R., Malik, M. R., Hernández-Pérez, F. E., and Im, H. G., *Proc. Combust. Inst.* 40: 105736,

(2024).

[39] Peters, N., *J. Fluid Mech.* 384: 107–132 (1999).

[40] Skiba, A. W., Wabel, T. M., Carter, C. D., Hammack, S. D., Temme, J. E., and Driscoll, J. F., *Combust. Flame* 189: 407–432 (2018).

[41] Fan Q., *et al.*, *Combust. Flame* 238: 111943 (2022).

[42] Mohammadnejad, S., An, Q. , Vena, P., Yun, S., and Kheirkhah, S., *Combust. Flame* 222: 285–304, (2020).

[43] Lawes, M., Ormsby, M. P., Sheppard, C. G. W., and Woolley, R., *Combust. Flame* 159: 1949–1959 (2012).

[44] Shy, S. S., Liu, C. C., Lin, J. Y., Chen, L. L., Lipatnikov, A. N., and Yang, S. I., *Proc. Combust. Inst.* 35: 1509–1516 (2015).

[45] Chaudhuri, S., Wu, F., and Law, C. K., *Phys. Rev. E* 88: 33005 (2013).

[46] Wu, F., Saha A., Chaudhuri, S., and Law, C. K., *Proc. Combust. Inst.* 35: 1501–1508 (2015).

[47] Lipatnikov A., and Chomiak, J., *Proc. Combust. Inst.* 31: 1361–1368 (2007).

[48] Wang, S., Elbaz, A. M., Wang, Z., and Roberts, W. L., *Combust. Flame* 232: 111521 (2021).

[49] Kitagawa, T., Nakahara, T., Maruyama, K., Kado, K., Hayakawa A., and Kobayashi, S., *Int. J. Hydrogen Energy* 33: 5842–5849 (2008).

[50] Bradley, D., Lau, A. K. C., and. Lawes, M, *Philos. Trans. R. Soc. London. Ser. A Phys. Eng. Sci.* 338: 359–387 (1992).

[51] Jiang, L. J., Shy, S. S., Li, W. Y. , Huang, H. M., and Nguyen, M. T., *Combust. Flame* 172: 173–182, (2016).

[52] Yu, R., and Lipatnikov, A. N., *Phys. Fluids* 29 (2017).

[53] Qu, Z., Wang, Y., Chen, X., and Chen, Z., *Fuel* : 378 132936 (2024).

[54] Glaznev, R., *et al.*, *Proc. Combust. Inst.* 40 105334 (2024).

[55] Zitouni,S., Brequigny, P., and Mounaïm-Rousselle, C., *European Combustion Meeting* (2023).